*PHYSOR 2004 -The Physics of Fuel Cycles and Advanced Nuclear Systems: Global Developments*
Chicago, Illinois, April 25-29, 2004, on CD-ROM, American Nuclear Society, Lagrange Park, IL. (2004)

# OECD/NEA International Benchmark on 3-D VENUS-2 MOX Core Measurements

Nadia Messaoudi[*1] and Byung-Chan Na[2]
[1]*SCK•CEN, Boeretang 200, B-2400 Mol, Belgium*
[2]*OECD/NEA, Le Saint-Germain, 12 Bd des Iles, 92130 Issy-les-Moulineaux, France*

For validating the calculation methods and nuclear data used for the prediction of power in MOX-fuelled systems, a series of theoretical physics benchmarks and multiple recycling issues of various MOX-fuelled systems have been addressed by the OECD/NEA. This led to many improvements and clarifications in nuclear data libraries and calculation methods. The final validation requires linking those findings to data from experiments. Hence, the first experiment-based benchmarks using the VENUS-2 MOX core measurement data have been started since 1999. The two-dimensional benchmark was completed in 2000. Overall, the results were very encouraging and confirmed that present methods using the latest nuclear data sets can adequately calculate MOX-fuelled systems. However, the calculation overestimated fission rates of MOX pins and slightly underestimated those of $UO_2$ pins. A full three-dimensional benchmark using 3-D VENUS-2 MOX core experimental data was therefore launched in 2001 for a more thorough investigation of the calculation methods. Twelve participants contributed to the 3-D benchmark, providing more than 20 solutions. This paper provides a summary of the comparison analysis of the 3-D calculation results against experimental data. Results obtained with the latest nuclear data libraries and various modern 3-D calculation methods are analyzed.

***KEYWORDS: VENUS-2 experiments, MOX fuel, three-dimensional calculations, axial pin power measurements, benchmark***

## 1. Introduction

Within the framework of the Nuclear Science Committee of the OECD/NEA, theoretical physics benchmarks and multiple recycling issues of various MOX-fuelled systems have been addressed. From the results of theoretical benchmarks performed, many improvements and clarifications in nuclear data libraries and calculation methods have been achieved. However, it was also felt that there was a need to link these findings to data from experiments. Hence, a blind international benchmark exercise based on the two-dimensional VENUS-2 MOX core measurement data was launched in 1999 and was completed in 2000 [1]. Overall, the results were very encouraging and confirmed that present methods using the latest nuclear data sets can adequately calculate MOX-fuelled systems. However, the calculation overestimated fission rates of MOX pins and slightly underestimated those of $UO_2$ pins.

A three-dimensional VENUS-2 MOX core benchmark was therefore launched in 2001 for a more thorough investigation into the calculation methods used for MOX-fuelled systems [2]. In the 3-D VENUS-2 measurements, the fission rate distributions of six fuel pins (two of each fuel type) in the core were measured by γ-scanning at 21 different axial levels [3]. The main objective of the benchmark is to calculate the axial fission rates of the 6 fuel pins to be compared with the measured values.

[*] Corresponding author, Tel.+32-14-332223, Fax +32-14-321529, E-mail: nmessaou@sckcen.be

Twelve participants contributed to the 3-D benchmark, providing more than 20 solutions. The calculated axial pin power distributions were compared with the experimental results.

Various nuclear data sets such as ENDF/B-IV, ENDF/B-VI, JEF-2.2, JENDL-3.2 and JENDL-3.3 were investigated. For axial power distribution calculations, four participants used the deterministic codes such as TORT, DANTSYS and PARCS and eight participants applied continuous energy Monte Carlo codes such as MCNP-4B, MCNP-4C, MVP and MCU-REA and a multigroup Monte Carlo code MOCA. This paper provides a summary of the comparative analysis between calculated and measured results. The detailed analysis and results can be found in Ref. [4].

## 2. Benchmark Model

The VENUS facility is a zero power critical PWR mock-up located at SCK•CEN in Belgium. As shown in Figure 1, the VENUS-2 core comprises 12 "15 × 15" subassemblies, instead of the "17 × 17" type (the pin-to-pin pitch remains typical of the "17 × 17" subassembly). The central part of the core (four 15 × 15 assemblies) consists of fuel pins 3.3 wt.% enriched in $^{235}$U. There are five Pyrex pins in 1/8 of the core. Of the eight assemblies on the periphery of the core, all of which contain fuel pins 4.0 wt.% enriched in $^{235}$U, eight rows of the most external fuel pins were replaced by mixed-oxide fuel pins ($UO_2$-$PuO_2$) enriched 2.0 wt.% in $^{235}$U and 2.7 wt.% in high grade plutonium.

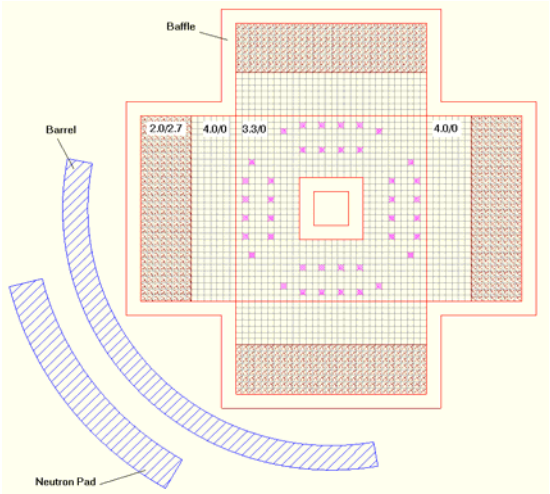


**Fig. 1** Horizontal cross-section of the VENUS-2 core geometry

Figure 2 shows a vertical cross-section of the core with corresponding axial co-ordinates. The core may be divided vertically, from bottom to top, in 10 parts:

- the *reactor vessel* (stainless steel)
- the *lower filling* (water),
- the *reactor support* (water and stainless steel, not shown in the figure),
- the *bottom grid* (32.8 vol % water and 67.2 vol % stainless steel*),
- the *lower reflector* (mainly water and Plexiglas); the reflector composition changes a little from one fuel region to another, depending on the structure of the corresponding fuel pins,
- the *active height* (fuel and stainless steel),

* The given composition values assume that no pin is loaded.

- the *upper reflector* (mainly water and Plexiglas), including the *intermediate grid* (63.4 vol % water and 36.6 vol % Plexiglas*); the reflector composition changes a little from one fuel region to another, depending on the structure of the corresponding fuel pins,
- the *upper grid* (63.4 vol % water and 36.6 vol % stainless steel*),
- the *upper filling* (water), and
- the VENUS room environment (air).

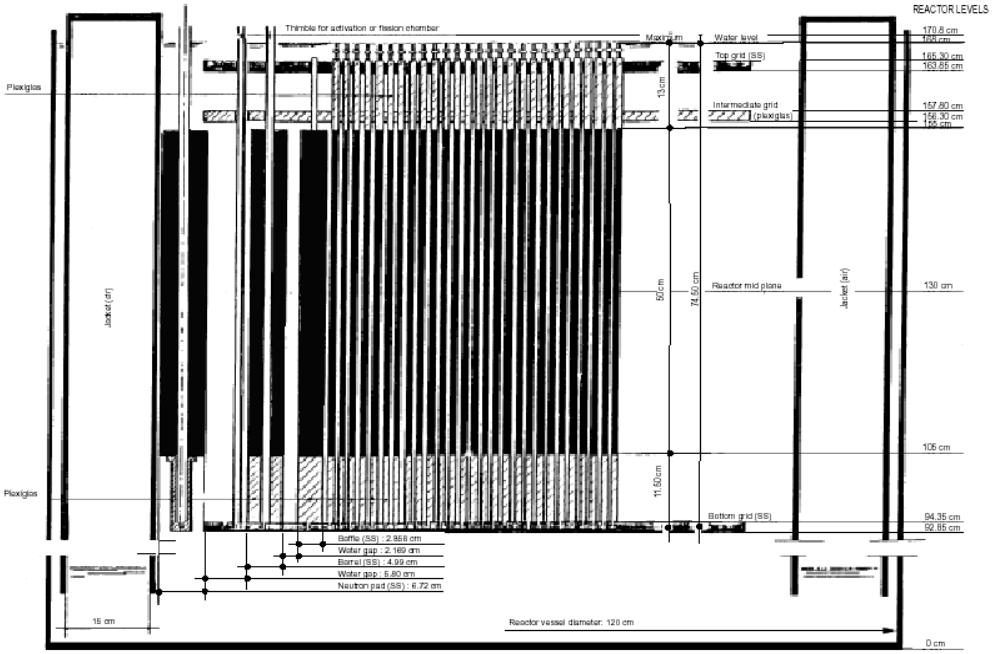


**Fig. 2** Vertical cross-section of the VENUS-2 reactor configuration

In the pin power measurements, one hundred and twenty-eight (128) fuel rods at the *mid-plane* of the core were measured after an irradiation of 13.5 h at 90% of the VENUS maximum power. One-eighth of the core comprises 325 fuel rods in which the pin powers of 121 fuel rods were directly measured and the pin powers of 204 fuel rods were interpolated from the measured values. The additional seven fuel pins measured were located in symmetric positions out of 1/8 of the core. The measured and interpolated positions of the fuel pins are shown in Figure 3. The pin power values were taken from the measured gamma activity of the $^{140}$La and normalized to a core averaged fission rate = 1 fission/sec/fuel cell. The average fission rate in the core corresponding to absolute reference irradiation is 1.87E+08 fissions/cm/sec at the mid-plane. This average fission rate corresponds to a power of 595 watts.

In addition, the fission rate distributions of six fuel pins (*two* $UO_2$ 3/0, *two* $UO_2$ 4/0 and *two* MOX 2/2.7 pins) were measured **axially** by γ-scanning after an irradiation of 8 h at 90 % of the VENUS maximum power. It originally was in order to obtain vertical buckling representative of the core. These three-dimensional pin power measurement results are the subject of this benchmark.

In the VENUS-2 experiments, the co-ordinates of the measurement points can be expressed in two different co-ordinate systems: (x,y) co-ordinates *with respect to the reactor grid* and (x,y) or (r,θ) co-ordinates *with respect to the core centre*.

* The given composition values assume that no pin is loaded.

According to the (x,y) co-ordinates with respect to the reactor grid, the axially measured 6 pin positions are (-27, -12), (-22, -2), (-15, +2), (-13, -12), (-11, +2) and (-6, -6). If the (x,y) co-ordinates with respect to the core centre are used, they are in the points (-37.17, +18.27), (-30.87, +5.67), (-22.05, +0.63), (-19.53, +18.27), (-17.01, +0.63) and (-10.71, +10.71) in cm. These axially measured 6 pin positions are shown in Figure 3 and their corresponding position numbers are 30, 74, 115, 131, 240 and 325.

The axial measurements were carried out at 21 different vertical planes along 50 cm of the fuel pin length (from 105 cm to 155 cm): starting from 110 cm, and at every 2 cm upwards to 150 cm.

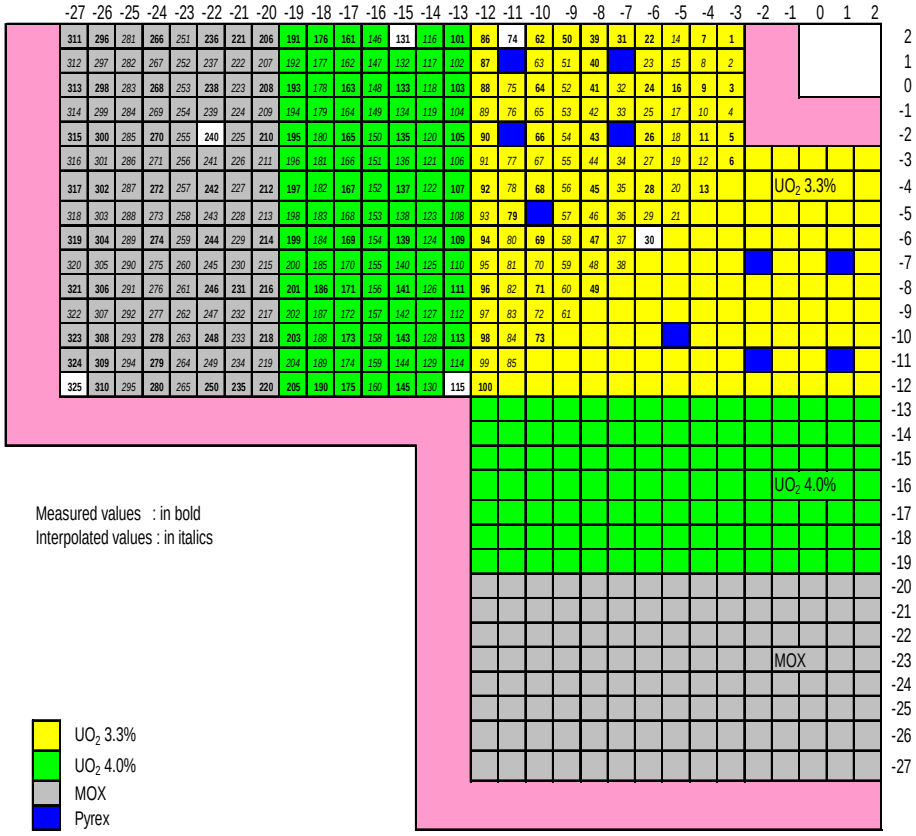


**Fig. 3** Measured and interpolated pin power positions in VENUS-2

Along with all geometry and material data required to develop the detailed computational model of the 1/4 fraction of the VENUS-2 reactor core, the isotopic concentrations of each medium were provided to the participants to minimize the discrepancies of the atomic density calculations [2].

From each fuel cell calculation ($UO_2$ 3.0, $UO_2$ 4.0, MOX), $k_\infty$, absorption and fission reaction rates per isotope (energy integrated and in three groups involving the 5 keV and 4 eV boundaries) were requested. From core calculations, it was requested to report $k_{eff}$ and normalized pin power (i.e. fission rate) distribution on 1/8 of the core which consists of 325 fuel pins (normalization was to be made to a core average fission rate = 1 fission/sec/fuel cell) and normalized axial fission rates of the six fuel pins. In this paper, a summary of the calculated results of $k_{eff}$ and of axial pin power distributions of the 6 fuel pins is presented.

## 3. Participants, Codes and Data Used, and Core Calculation Methods Applied

Twelve participants contributed to the benchmark, providing more than 20 solutions. The complete list of participants, basic libraries and codes used are presented in Table 1 below.

**Table 1** Participants, basic library and computer codes used

| Institution (Country) | Participants | Codes used | Data used | Energy group |
|---|---|---|---|---|
| **FRAMATOME-ANP (Germany)** | W. Hofmann<br>J. Koban<br>W. Timm | CASMO-4<br>TORT-2.7.3 | ENDF/B-IV<br>(Er and Tm data from JEF-1 and JEF-2.1) | 5 groups |
| **KAERI (Korea)** | D.H. Kim<br>J.D. Kim<br>C.S. Gil<br>J.H. Chang | TRANSX-2.15<br>DANTSYS-3.0 | ENDF/B-VI.7<br>(Sn from ENDL84) | 35 groups |
| **NEA + KAERI (Korea)** | B-C. Na (NEA)<br>G.H. Roh (KAERI) | TRANSX-2.15<br>TORT-3.2 | ENDF/B-VI.5<br>JENDL-3.2 | 35 groups |
| **Purdue Univ. (USA)** | T. Kozlowski<br>C.H. Lee<br>T.J. Downar | HELIOS-1.7<br>PARCS-2.1 | ENDF/B-VI.3 | 8 groups |
| **FRAMATOME-ANP (Germany)** | W. Timm<br>S. Misu<br>D. Porsch | CASMO-4<br>MOCA | ENDF/B-IV<br>(Er and Tm data from JEF-1 and JEF-2.1) | Multi-group Monte Carlo:<br>5 groups |
| **JAERI (Japan)** | Y. Nagaya<br>K. Okumura<br>T. Mori | MVP | JENDL-3.2<br>(Sn from CENDL-2)<br>JENDL-3.3<br>(S, Si, Mo from JENDL-3.2 and Sn from CENDL-2) | Continuous |
| **SCK•CEN (Belgium)** | N. Messaoudi<br>H.Aït Abderrahim | MCNP-4C | ENDF/B-VI.5<br>JEF-2.2 | Continuous |
| **KAERI (Korea) + NEA** | G.H. Roh (KAERI)<br>B-C. Na (NEA) | MCNP-4B | ENDF/B-VI.5<br>JENDL-3.2<br>JEF-2.2 | Continuous |
| **KFKI (Hungary)** | G. Hordósy | MCNP-4C | ENDF/B-VI.2<br>(structural material data from ENDF/B-V) | Continuous |
| **KI (Russia)** | E. Gomin<br>M. Kalugin | MCU-REA | MCU data library<br>(based on ENDF/B-VI, JENDL-3.2 and BROND) | Continuous |
| **GRS+IKE (Germany)** | W. Zwermann (GRS)<br>M. Mattes (IKE) | MCNP-4C | ENDF/B-VI.5<br>JENDL-3.2<br>JEF-2.2 | Continuous |
| **SEA (Spain)** | D.L. Maganto | MCNP-4C | ENDF/B-VI for fuel, water, some elements of steel structures (for the rest from ENDF/B-V) | Continuous |

As for core calculation methods and models applied, all participants provided their calculation details [4]. These are summarised below.

FRAMATOME-ANP GmbH used both the deterministic $S_N$ code TORT and the multi-group Monte Carlo code MOCA. In both TORT and MOCA core calculations, the uniform grid with a pitch of 1.26 cm in x-y direction has been preserved in all regions outside the fissile zones, i.e. baffle, water, barrel. Therefore, baffle, barrel and neutron pad have been modelled only approximately in this uniform grid, i.e. in such a way that the masses (areas) of these materials are approximately preserved. In the geometrical model a size of $55 \times 55$ "meshes" has been assumed in the x-y direction. The geometrical model was limited to a core quadrant. Axially, only two additional materials have been introduced: (1) rods with Plexiglas (surrounded by water) above and below the 3/0 $UO_2$ zone and (2) rods with Plexiglas (surrounded by water) above and below the 4/0 $UO_2$ zone and the 2/2.7 MOX zone.

In TORT calculations for the upper axial reflector a thickness of 13 cm has been assumed and for the lower a thickness of 21.5 cm. For these regions a combination of Plexiglas and water zones has been used. The 3-D TORT calculations were performed in x-y-z geometry with $S_8P_0$ approximation. For comparison with the $S_8$ calculation an extra $S_2$ calculation was performed. In order to obtain an accurate axial power profile in the specified fuel rods, the rods were split axially into 25 equidistant regions (2 cm per region). All results have been obtained by assuming quarter core symmetry.

In MOCA calculations, all grid plate materials have been neglected. For the upper axial reflector a thickness of 13 cm has been assumed and for the lower a thickness of 30 cm. In order to obtain a sufficiently accurate axial power profile in the specified fuel rods, these were split axially into seven almost equidistant regions (around 7 cm per region) and the axial fission rate distribution was then calculated by a simple spline interpolation preserving the rates of these seven axial zones. Since no statistically significant axial asymmetry was detected, axial profiles were symmetrised. All results have been obtained by assuming quarter core symmetry. Comparisons with full core calculations (taking into account the barrel and neutron pad only in one quarter of the core) gave a $k_{eff}$ which seemed to be around 20 to 30 pcm lower than the symmetrical core (high statistical uncertainty here), so the presence of the barrel seems to slightly increase the $k_{eff}$. However the pin power distribution was not affected with full core geometry (no statistically significant effects were detected).

KAERI used the 3-D $S_N$ code THREEDANT in the DANTSYS 3.0 system and NEA+KAERI applied the 3-D $S_N$ code TORT in the DOORS 3.2 system. Both calculations applied $S_8P_3$ approximation for angular descretisation. In KAERI calculations, the mesh sizes were less than ~0.03 cm for three fuel cells. The VENUS-2 core was modelled explicitly from bottom to top with the proper use of homogenisation for the grid regions and the core was modelled up to the barrel in the x- and y-direction. The regions beyond the barrel were filled with water and the neutron pad was not taken into account. In NEA+KAERI calculations, one quarter of the full 3-D VENUS-2 core was modelled with $100 \times 102 \times 72$ spatial meshes in the (x,y,z) geometry. Fully symmetrical quadrature sets were introduced. The point-wise flux convergence criterion used was 1.0E-4 and the eigenvalue convergence criterion applied was 1.0E-5.

In Purdue University core calculations, the PARCS core simulator was applied using fine mesh finite difference $SP_3$ kernel with one mesh per pin cell and SPH factors. Fuel and radial reflector cross-sections and corresponding SPH factors were generated from a VENUS-2 2-D HELIOS solution. Axial reflector cross-sections and SPH factors were generated from a 1-D homogeneous fuel-heterogeneous reflector HELIOS solution.

For JAERI MVP calculations, a quarter-symmetric core model was developed. This model included lower filling, reactor support, bottom, intermediate and upper grids, top and bottom reflectors, top and bottom stops and upper filling axially. It also included reactor vessel, jacket, neutron pad, barrel, outer

and inner baffles radially. The neutron pad was assumed to be a part of a cylindrical tube, though the real pad does not have uniform thickness. A full-core calculation was performed to investigate the asymmetric effect of the barrel and neutron pad on the pin power distribution but no difference was seen between the full-core and quarter-symmetric models. Thus the quarter-symmetric model was employed to reduce statistical errors. No data were available for the top and bottom reflectors and tops for MOX pins. Thus the same data were assumed as for 4/0 $UO_2$ pins The scattering law $S(\alpha,\beta)$ of polyethylene was used for Plexiglas as no scattering law was available for this material. Tally regions for pin power distribution include not only the single unit cells of interest but also symmetric cells, though the geometry is not symmetric with regard to the diagonal due to the neutron pad. Histories for 3-D core calculation were 199 million: 9 950 cycles and 20 000 neutrons per cycle (not including 50 cycles for initial guess).

In SCK•CEN MCNP-4C core calculations, one quarter of the full 3-D core was explicitly modelled in three-dimensional geometry. All fuel rods and Pyrex rods were fully modelled including the fuel pellet, fuel gap in $UO_2$ pin cells, clad and coolant. The radial core components such as the reactor vessel, jacket, neutron pad, barrel, reflector, outer baffle, inner baffle and inner hole, etc., were also fully modelled. The core was modelled vertically from bottom to top, i.e. lower filling, reactor support, bottom grid, lower reflector, upper grid, upper filling, etc. In order to obtain the axial fission rate distributions in the core, the core was divided into 25 axial layers. Since no thermal scattering data for Plexiglas (upper and lower reflectors) are available, one set of calculations was performed using the scattering data of polyethylene in place of Plexiglas and another set of calculations was undertaken which ignored the thermal scattering of axial reflectors. It was shown that the thermal scattering of the axial reflectors did not play an important role in calculated axial pin power results. Therefore, they were not taken into account in the final calculations. Three hundred fifty (350) million histories (500 000 neutrons per cycle with 700 cycles) were used.

In KAERI+NEA MCNP-4B calculations, one quarter of the full 3-D core was explicitly modelled. The number of histories originally used was $50 \times 10^6$ (100 000 neutrons/cycle and 500 cycles after 100 inactive cycles) as a reference calculation. To investigate the influence of the number of histories on calculated results, they were increased to $200 \times 10^6$ and then to $300 \times 10^6$ (100 000 neutrons/cycle and 3 000 cycles after 100 inactive cycles). The thermal scattering of Plexiglas was not taken into account.

GRS+IKE also developed one quarter of the 3-D core model. Forty (40) million histories were used (4 000 neutrons per cycle and 10 000 cycles). Since no $S(\alpha,\beta)$ data are available for Plexiglas, polyethylene data were used to describe the thermal scattering of the axial reflectors. Due to the neutron pad, the arrangement is not totally symmetric with regard to the diagonal; each pin fission rate value was therefore calculated by taking the average of pins (i,j) and (j,i).

KFKI, KI and SEA provided no details on calculation models and assumptions. However, it is believed that they developed 1/4 of the full 3-D core model. In KFKI MCNP-4C calculations, for the axial power distribution calculations, the pins were divided into 2-cm high cells, and the volume averaged fission rate of these segments was used. Thirty-seven (37) million histories were used. In KI MCU-REA calculations, 40 million histories were used. No specific assumptions for the calculation model were made, but the neutron pad outer radius used was 65.073 cm instead of the value given in the specification. In SEA MCNP-4C calculations, 40 million neutron histories were used for all calculations, but for the axial fission rates in the MOX zone, 60 million neutron histories were used.

## 4. Summary of Core Calculation Results

For the core calculations, $k_{eff}$, normalised radial fission rate distribution at 325 fuel pin positions at the code mid-plane, and normalised axial fission rate distribution of six fuel pins were requested. However, in this paper, the analysis is focused on $k_{eff}$ and axial fission rate distributions of six fuel pins.

For the following analysis, it is worth noting that the measured $k_{eff}$ value is 1 with an uncertainty of ±32 pcm, and that the reported uncertainties of the measured data (1σ) of pin power distributions of the six fuel pins are ±2.2% in $UO_2$ and ±3.4% in MOX pins.

### 4.1 Effective Multiplication Factor ($k_{eff}$)

The calculated $k_{eff}$ values are compared in Table 2. All reported $k_{eff}$ show in general a very good agreement with the experimental value ($k_{eff}$ = 1). The average $k_{eff}$ from all calculations is 1.00122±0.00394. The deterministic calculations produce an average of 0.99828±0.00402 and the Monte Carlo calculations lead to an average of 1.00232±0.00341. The maximum discrepancy reported is about 1% by the KAERI+NEA calculation with JENDL-3.2. This represents about 1 000 pcm of differences. The origin of this large discrepancy is not clearly understood, since no abnormal behaviour was observed in reaction rate results obtained by KAERI+NEA cell calculations with the JENDL-3.2 library. The other JENDL-3.2 based calculations report less than 0.5% of discrepancies. Deterministic calculation results show a trend of slight underestimation of $k_{eff}$ (but less than 0.5% in the most cases). Most of the Monte Carlo calculations reported $k_{eff}$ values with a discrepancy of less than 0.1%. Two JEF-based results reported by SCK•CEN and KAERI+NEA show discrepancies of about 0.7% whereas the GRS JEF-based result gives a discrepancy of less than 0.3%.

Between two versions of the JENDL library, JENDL-3.3 gives a better result than JENDL-3.2. However, no clear advantage of one library over the others was observed and no systematic dependency on basic libraries in $k_{eff}$ calculations was seen. Differences in reported $k_{eff}$ values would be due to different nuclear data processing procedures and the calculation models used. A further investigation into nuclear data processing procedures and calculation models used by the participants could better clarify the origin of the discrepancies observed in $k_{eff}$ result.

### 4.2 Axial Pin Power Distribution

#### 4.2.1 General Comparison

The calculated results were relatively compared against measured power distributions as (C/E)-1 in %. For the MOX pin (-27,-12), as presented in Figure 4, deterministic calculations show about ±2% of scatter band for most of the axial positions. However, the scatter band becomes larger near the axial lower and upper reflectors. Monte Carlo calculations presented in Figure 5 show a statistical perturbation giving a larger scatter band than deterministic calculations. For most of the axial positions, the scatter band is about ±3% and it becomes larger near the axial reflectors as in deterministic calculations. The large statistical perturbation in Monte Carlo calculations and a larger scatter band near the axial reflectors in both deterministic and Monte Carlo calculations might be partially due to the extreme position of the pin (-27,12), which is located next to the outer baffle. The Monte Carlo calculations that used a smaller number of particle histories show a more pronounced statistical perturbation.

**Table 2** $k_{eff}$ values of core calculations

| Institution | Code used | Library used | $k_{eff}$ | Statistical error (1σ) | Deviation (%) | Comments |
|---|---|---|---|---|---|---|
| FRAMATOME-ANP | TORT-2.7.3 | ENDF/B-IV | 0.99719 | – | -0.28 | $S_8P_0$ (5 groups) |
| | | ENDF/B-IV | 0.99438 | – | -0.56 | $S_2P_0$ (5 groups) |
| KAERI | DANTSYS-3.0 | ENDF/B-VI.7 | 0.99659 | – | -0.34 | $S_8P_3$ (35 groups) |
| NEA+KAERI | TORT-3.2 | ENDF/B-VI.5 | 0.99549 | – | -0.45 | $S_8P_3$ (35 groups) |
| | | JENDL-3.2 | 1.00511 | – | 0.51 | $S_8P_3$ (35 groups) |
| Purdue Univ. | PARCS-2.1 | ENDF/B-VI.3 | 1.00093 | – | 0.09 | (8 groups) |
| FRAMATOME-ANP | MOCA | ENDF/B-IV | 1.00110 | 0.00007 | 0.11 | 5 groups, histories? |
| JAERI | MVP | JENDL-3.2 | 1.00500 | 0.000055 | 0.50 | Histories: 199 million |
| | | JENDL-3.3 | 1.00056 | 0.000054 | 0.06 | Histories: 199 million |
| SCK•CEN | MCNP-4C | ENDF/B-VI.5 | 1.00062 | 0.00004 | 0.06 | Histories: 350 million |
| | | JEF-2.2 | 1.00662 | 0.00004 | 0.66 | Histories: 350 million |
| KAERI+NEA | MCNP-4B | ENDF60 | 1.00036 | 0.00014 | 0.04 | Histories: 50 million |
| | | ENDF60 | 1.00046 | 0.00007 | 0.05 | Histories: 200 million |
| | | ENDF60 | 1.00056 | 0.00006 | 0.06 | Histories: 300 million |
| | | ENDF/B-VI.5 | 1.00199 | 0.00007 | 0.20 | Histories: 200 million |
| | | JENDL-3.2 | 1.01014 | 0.00007 | 1.01 | Histories: 200 million |
| | | JEF-2.2 | 1.00747 | 0.00007 | 0.75 | Histories: 200 million |
| KFKI | MCNP-4C | ENDF/B-VI.2 | 0.99880 | 0.00013 | -0.12 | Histories: 37 million |
| KI | MCU-REA | MCUDAT | 0.99946 | 0.00015 | -0.05 | Histories: 40 million |
| GRS+IKE | MCNP-4C | ENDF/B-VI.5 | 0.99794 | 0.00012 | -0.21 | Histories: 40 million |
| | | JENDL-3.2 | 1.00369 | 0.00012 | 0.37 | Histories: 40 million |
| | | JEF-2.2 | 1.00275 | 0.00012 | 0.28 | Histories: 40 million |
| SEA | MCNP-4C | ENDF/B-VI | 1.00028 | 0.00012 | 0.03 | Histories: 40 million (60 million for MOX zone) |

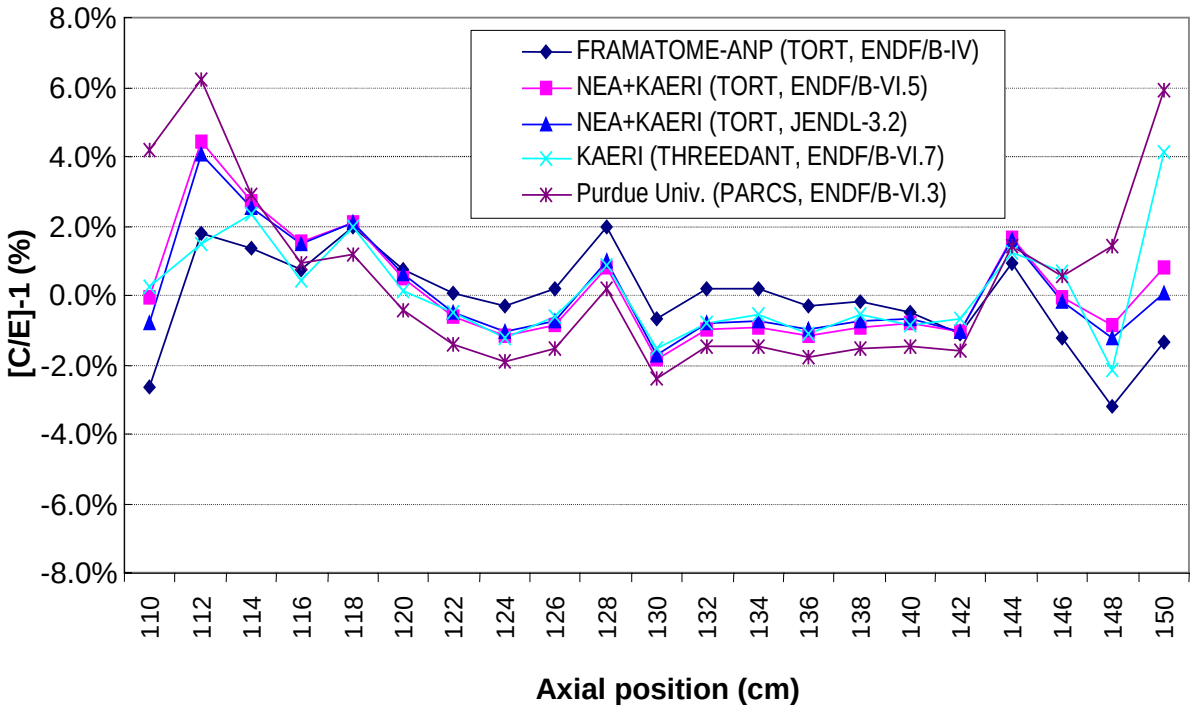


**Fig. 4** Deterministic calculations: Comparison of axial power distributions in MOX pin (-27,-12)

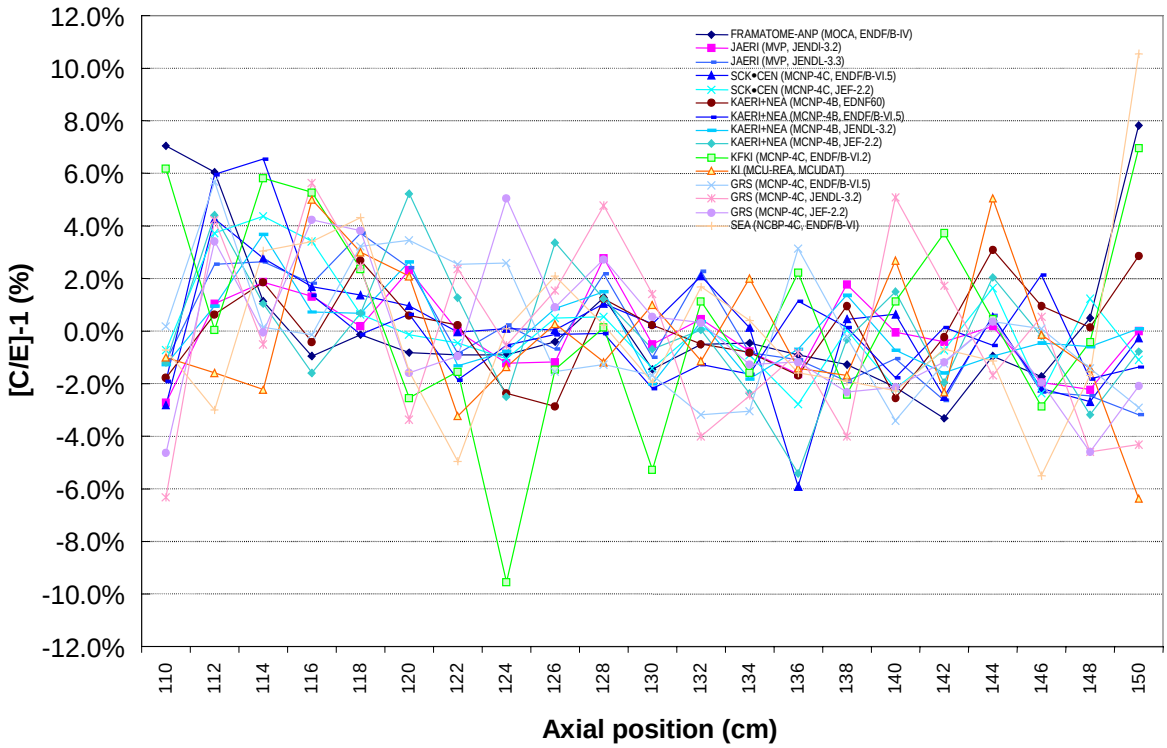


**Fig. 5** Monte Carlo calculations: Comparison of axial power distributions in MOX pin (-27,-12)

For the MOX pin (-22,-2), deterministic calculation results give about ±2% of scatter band for most of the axial positions. Larger discrepancies near the axial reflectors are still observed in the pin (-22,-2),

however these are less pronounced in the pin (-22,-2) than in the pin (-27,-12). All five calculation results reported more than 4% of discrepancy for the axial position at 116 cm. Monte Carlo calculations give better results for this pin than for the pin (-27,-12) and show less statistical perturbation. The scatter band is about ±2% for most of the axial positions. As in deterministic calculations, most of the Monte Carlo calculations reported more than 4% of discrepancy for the axial position at 116 cm. The accuracy of the measurement for this position may be doubtful.

For the 4/0 $UO_2$ pin (-15,+2), an excellent agreement is observed in the results obtained by deterministic calculations (see Figure 6). For most of the axial positions, the scatter band is less than ±1%. Near the upper axial reflector, the scatter band becomes a bit larger (about 3%). The same trend is observed in Monte Carlo calculation results (see Figure7). A slightly larger scatter band is seen in some Monte Carlo calculation results, probably due to their statistical perturbation. Again, as in deterministic calculations, near the upper axial reflector, the scatter band becomes larger, up to 2-4%. Most of the Monte Carlo results show a very similar profile of pin powers, however some results seem to suffer from a more pronounced statistical perturbation. This might be simply the question of the total number of particle histories used, and could be corrected by increasing the number of histories.

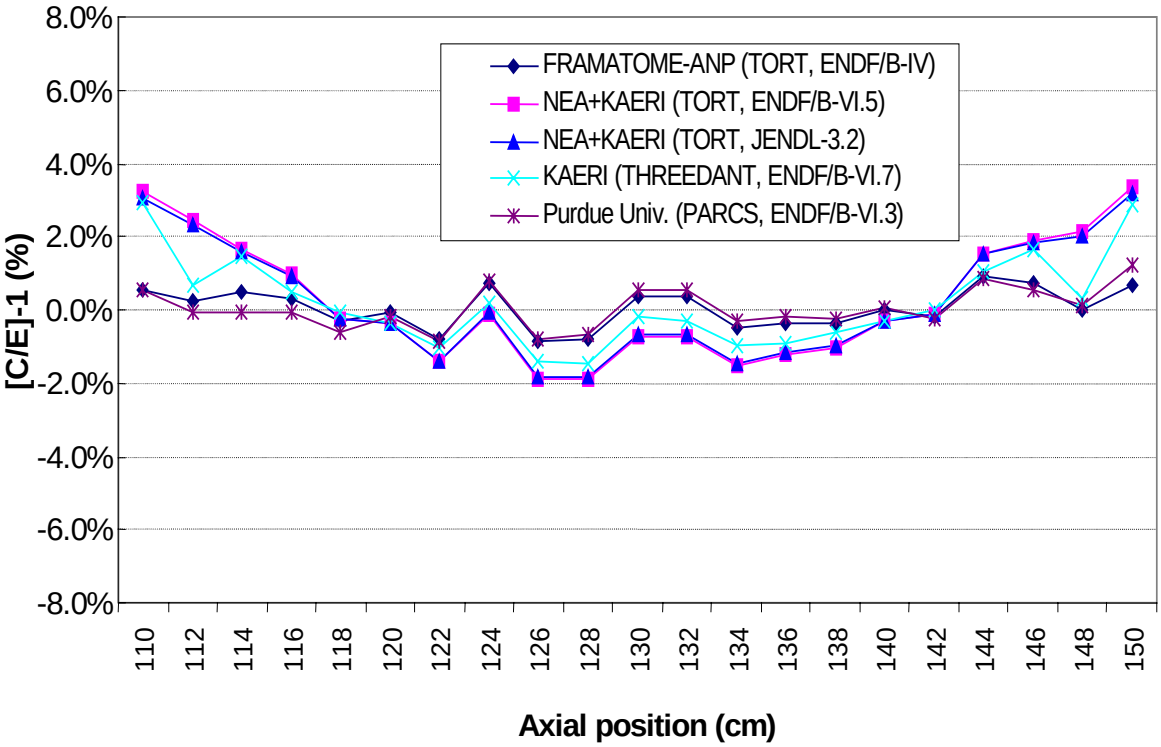


**Fig. 6** Deterministic calculations: Comparison of axial power distributions in 4/0 $UO_2$ pin (-15,+2)

For the 4/0 $UO_2$ pin (-13,-12), deterministic calculation results show an excellent agreement with experimental results. For most of the axial positions, the scatter band is between almost 0 and 1%. However, a trend of slight overestimation of pin powers is observed near the lower and upper axial reflectors. Monte Carlo calculations also report a good agreement giving a scatter band of less than ±2% for most of the axial positions. A trend of slightly overestimating of the pin powers near the axial reflectors is observed. FRAMATOME-ANP MOCA results give highly overestimated pin powers for the positions at 110 cm and 150 cm. This problem could be the result of a rough extrapolation of pin powers at the boundaries in MOCA calculations (the axial meshes used in MOCA fission rate calculations were larger than 2 cm) and this could be remedied by a better extrapolation.

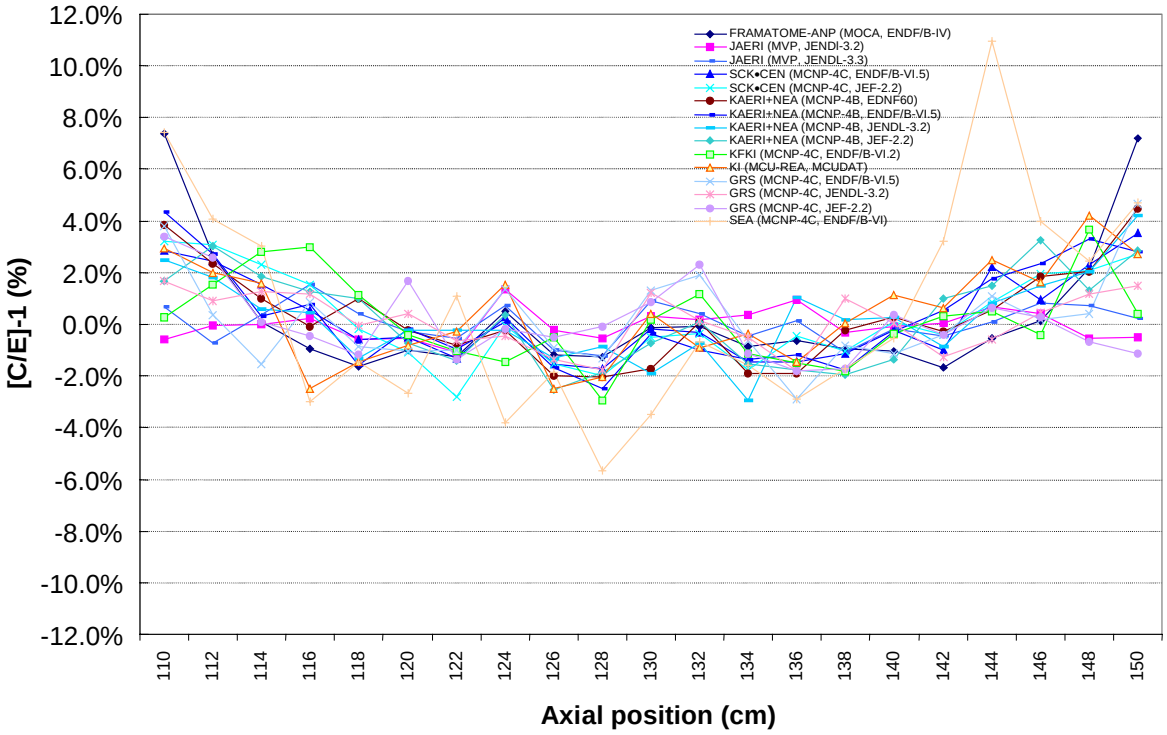


**Fig. 7** Monte Carlo calculations: Comparison of axial power distributions in 4/0 $UO_2$ pin (-15,+2)

The 3/0 $UO_2$ pin (-11,+2) is located next to a Pyrex pin which contains the absorbing material. Both deterministic and Monte Carlo calculation results show almost the same profile of pin powers (see Figures 8 and 9). For the axial positions in the middle, the scatter band is less than or about ±1% from deterministic calculations and about ±1% from Monte Carlo calculations. A trend of slight overestimation of pin powers is observed at positions near the lower and upper axial reflectors. No noticeable influence of the Pyrex pin on calculated pin powers is observed.

For the 3/0 $UO_2$ pin (-6,-6), deterministic calculations report less than ±1% of scatter band and Monte Carlo results about ±1% for most of the axial positions in the central part of the pin, as in the pin (-11,+2). However, a slight overestimation at positions near the upper reflector and a slight underestimation of pin powers at positions near the lower reflector region in both deterministic and Monte Carlo calculation results are observed.

### 4.2.2 Comparison of Libraries

JAERI applied two versions of the JENDL library (3.2 and 3.3). SCK•CEN used two libraries based on ENDF/B-VI.5 and JEF-2.2. Both KAERI+NEA and GRS examined three libraries based on ENDF/B-VI.5, JENDL-3.2 and JEF-2.2. In addition, KAERI+NEA also applied the MCNP-4B package library ENDF60.

Due to the fact that all Monte Carlo results show the statistical perturbation and that for some positions one library gives a better result, but worse results for other positions with other libraries, an absolute comparison of results with different libraries is not possible. The accuracy of pin power results seem to be more dependent on how the core is modelled and how the cross-sections are prepared.

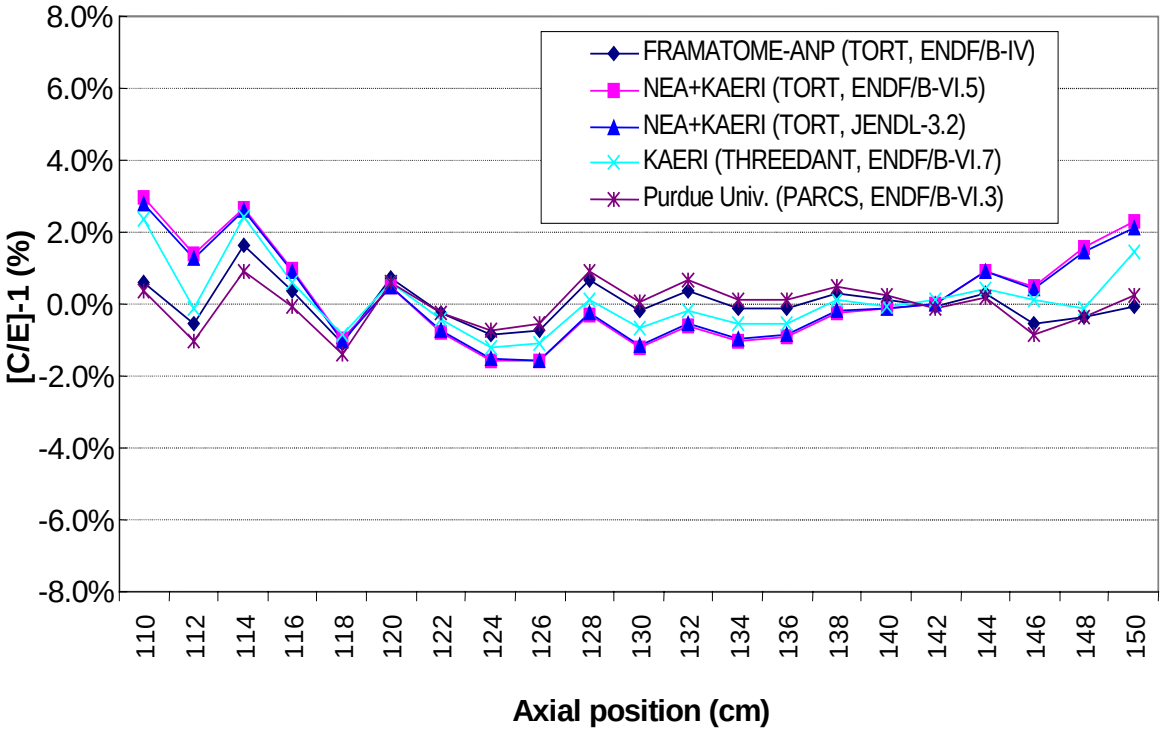


**Fig. 8** Deterministic calculations: Comparison of axial power distributions in 3/0 $UO_2$ pin (-11,+2)

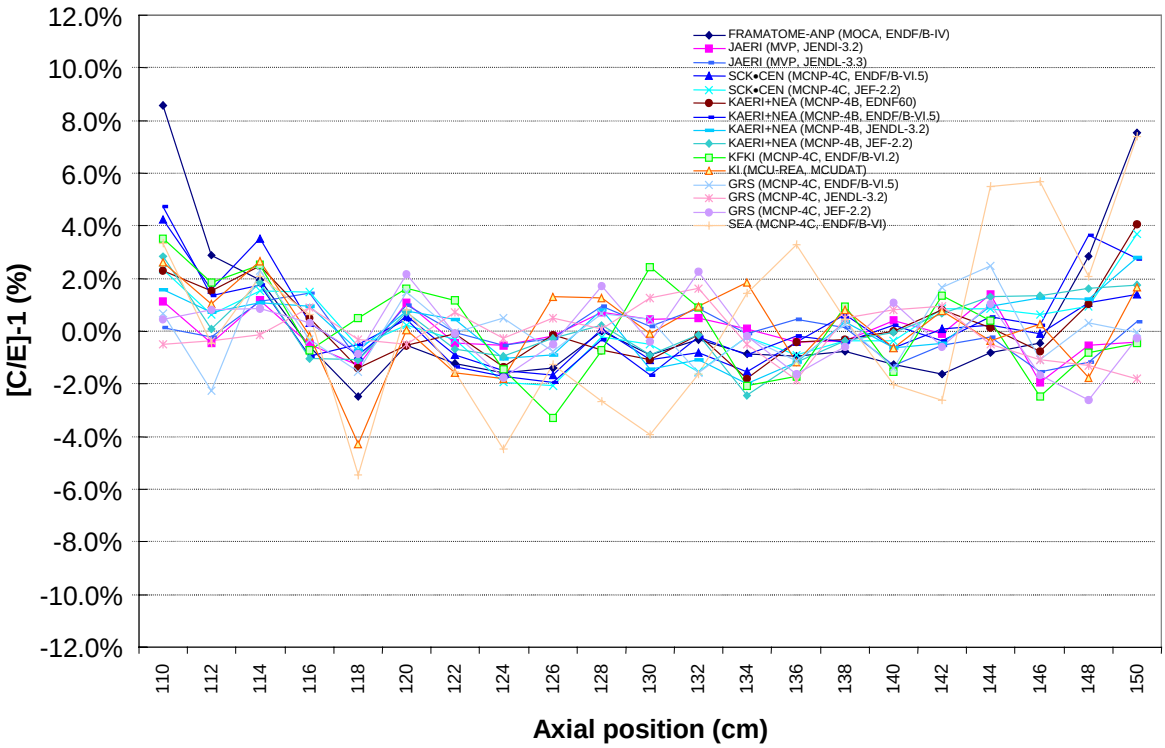


**Fig. 9** Monte Carlo calculations: Comparison of axial power distributions in 3/0 $UO_2$ pin (-11,+2)

### 4.2.3 Comparison of Number of Particle Histories

KAERI+NEA performed a series of supplementary calculations to investigate the influence of the number of particle histories on the accuracy of pin power results. For this, all the calculations were carried out with the MCNP package library ENDF60, increasing the number of histories for each step. The reference case was undertaken with $50 \times 10^6$ of histories (100 000 neutrons/cycle and 500 cycles after 100 inactive cycles). However, the calculation model does not take into account the top and bottom stops of the active fuel pins and top and bottom blankets in the axial reflector regions, which might cause larger discrepancies of pin powers near the axial reflectors.

When the number of histories is increased to $200 \times 10^6$ (100 000 neutrons/cycle and 2 000 cycles after 100 inactive cycles), the relative errors ($1\sigma$) are about 1.8% for the MOX pin (-27,-12) and about 1.0% for the MOX pin (-22,-2), while they are about 0.7% for the four $UO_2$ pins. In consequence, the scatter bands become much smaller for both MOX and $UO_2$ pins than in the reference calculation with $50 \times 10^6$ histories. However, larger discrepancies near the axial reflectors are still observed, especially for the $UO_2$ pins. For the MOX (-27,-12) pin, all 21 axial positions give a discrepancy of less than 3.4%, which is the reported uncertainty of the measurement. In the MOX (-22,-2) pin, 18 positions out of 21 show about or less than 2%. In the $UO_2$ pins, for most of the axial positions (18 positions for the 4/0 $UO_2$ and 19-20 for $UO_2$ 3/0 pins), the agreements between calculated and measured pin power values are very good (less than ±2%). The slightly worse results for the $UO_2$ pins are due to the pronounced reflector effect near the axial upper and lower reflectors.

To examine more thoroughly the influence of the number of histories on results, the histories were again increased up to $300 \times 10^6$ (100 000 neutrons/cycle and 3 000 cycles after 100 inactive cycles). From the latter calculation, the reported relative errors ($1\sigma$) are about 1.5% for the MOX pin (-27,-12) and about 0.8% for the MOX pin (-22,-2), and they are about 0.6% for the four $UO_2$ pins. However, the pin power results obtained show almost the same trend as those from the calculations with $200 \times 10^6$ histories. Therefore, compared to the calculated results with $200 \times 10^6$ histories, no real advantage is obtained when the number of histories is increased to $300 \times 10^6$. As an example, the result for the 3/0 $UO_2$ pin (-11,+2) case is presented in Figure 10.

To summarise, some Monte Carlo calculation results that showed a statistical perturbation with the limited number of histories used might be improved to some extent if a sufficient number of histories were to be applied.

### 4.2.4 Comments on Pin Power Discrepancies Near the Axial Reflectors

With regard to somewhat larger discrepancies observed in $UO_2$ pins at axial positions near the upper and lower reflector regions, even though discrepancies are often within the reported measurement uncertainties in many calculation results, this could originate from the fact that most of the calculation models ignored the detailed structures above and below the active fuel pins, i.e. top and bottom stops of the active fuel pins and top and bottom blankets in the axial reflector regions.

JAERI took into account the detailed structures above and below the active fuel pins in its calculation model [4, 5] and JAERI results do not show pronounced discrepancies of pin powers observed in $UO_2$ pins at positions near the axial reflectors. It is therefore believed that ignoring detailed structures above and below the active fuel pins in the calculation model may cause about 1 or 2% of pin power discrepancy at axial positions near the axial reflectors.

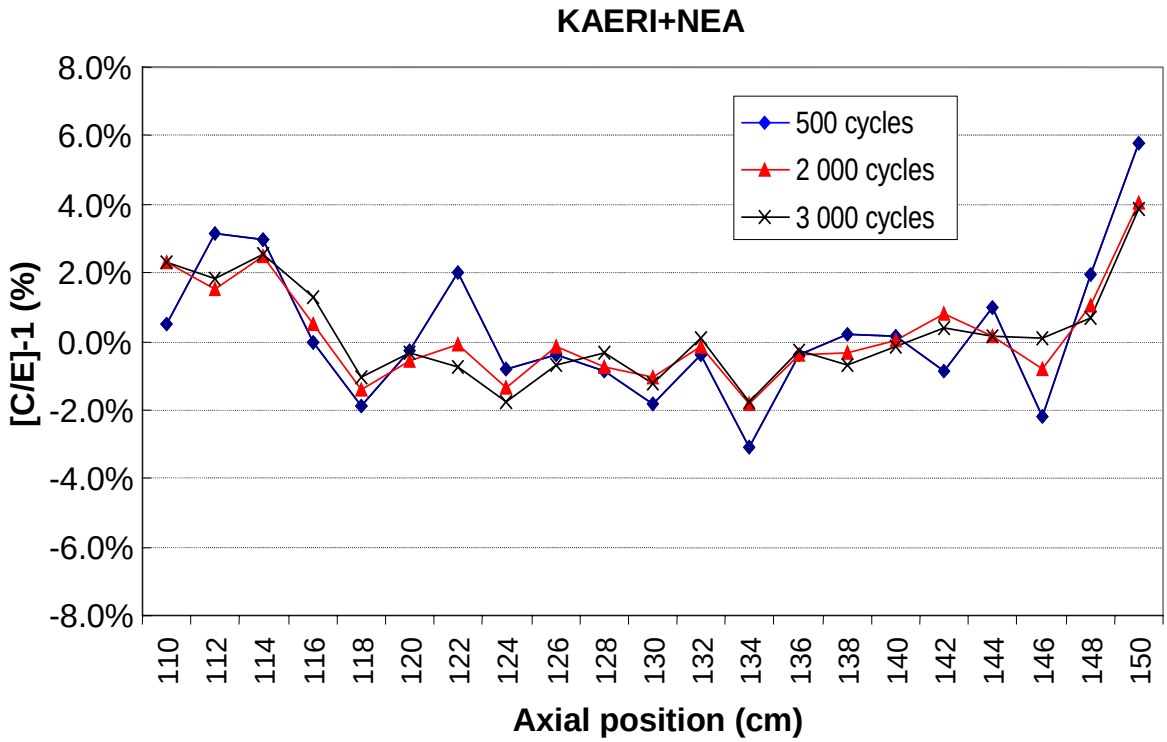


**Fig. 10** Comparison of number of particle histories for 3/0 $UO_2$ pin (-11,+2)

Moreover, according to the benchmark specification and the original document on the experiments provided by SCK•CEN, the reflector composition changes a little from one fuel region to another, depending on the structure of the corresponding fuel pins. However, the detailed information on these composition changes was not available and could not be given to the participants. Therefore, some approximations made by each participant to describe the lower and upper reflectors as a mixture of water, grid and Plexiglas would affect pin power results near the axial reflectors.

This will be further studied by performing supplementary calculations to quantify the influence of detailed axial structures on calculated pin powers near the axial reflectors.

Through a comparison calculation undertaken by SCK•CEN, it was found that ignoring the thermal scattering by Plexiglas, which is the main component of the axial reflectors, does not have an important influence on larger discrepancies observed at positions near the axial reflectors.

## 5. Conclusions

Following the two-dimensional VENUS-2 MOX core benchmark, an international benchmark exercise based on the three-dimensional VENUS-2 MOX core experiment results was organised by the OECD/NEA. The benchmark aimed at validating three-dimensional calculation methods together with the latest nuclear data used for MOX-fuelled systems. Therefore, the measured axial pin power distributions of the six fuel pins at 21 axial positions were main investigative purpose of the benchmark. Twelve participants contributed to the benchmark, providing more than 20 solutions. Various nuclear data sets such as ENDF/B-IV, several versions of ENDF/B-VI, JEF-2.2 and two versions of JENDL (3.2 and 3.3) were used. For core calculations predicting axial power distributions, four participants applied deterministic codes such as TORT, DANTSYS and PARCS, and eight participants used continuous-energy Monte Carlo codes such as MCNP-4B, MCNP-4C, MVP and MCU-REA, and the multi-group Monte Carlo code MOCA.

The analysis of results confirms that all combinations of the present methods using the latest nuclear data sets can adequately calculate MOX-fuelled systems in 3-D geometry, producing reasonably accurate axial pin power distributions.

With regard to somewhat larger discrepancies observed in $UO_2$ pins at axial positions near the upper and lower reflector regions, this could originate from the fact that most of the calculation models ignored the detailed structures above and below the active fuel pins, i.e. top and bottom stops of the active fuel pins and top and bottom blankets in the axial reflector regions. This will be further studied by performing supplementary calculations to quantify the influence of detailed axial structures on calculated pin powers near the axial reflectors.

The 3-D VENUS-2 MOX core experimental data provided by SCK•CEN were very useful for comparison of calculated results against them to investigate current methods and nuclear data. The reported uncertainties of the measured data ($1\sigma$) for the six fuel pins are $\pm 2.2\%$ in $UO_2$ and $\pm 3.4\%$ in MOX pins. Further studies using experimental data with smaller uncertainties would contribute to additional refinements of calculation methods used for MOX-fuelled systems.

**Acknowledgements**

The authors wish to thank all benchmark participants who willingly devoted their time and effort to this benchmark.

**References**

1) Byung-Chan Na, "Benchmark on the VENUS-2 MOX Core Measurements," OECD/NEA report, NEA/NSC/DOC(2000)7, ISBN 92-64-18276-4 (December 2000).

2) Byung-Chan Na and Nadia Messaoudi, "Blind Benchmark on the 3-D VENUS-2 MOX Core Benchmark,"Final Specification, NEA/SEN/NSC/WPPR(2001)1 (May 2001).

3) K. van der Meer, et al., "Additional Data for the 3-D VENUS-2 Benchmark," SCK•CEN report, TN-0008 (September 2000).

4) Nadia Messaoudi and Byung-Chan Na, "Benchmark on the Three-Dimensional VENUS-2 MOX Core Measurements," OECD/NEA report, NEA/NSC/DOC(2003)5 (January 2004).

5) Y. Nagaya, K. Okumura and T. Mori, "Analysis of VENUS-2 MOX Core Measurements with a Monte Carlo Code MVP," *Proc. Int. Conf. On the New Frontiers of Nuclear Technology: Reactor Physic, Safety and High Performance Computing (PHYSOR 2002)*, Seoul, Korea, 7-10 October 2002, 4A-04 (2002).